

# Measuring motion of vulnerable road users relative to moving HGVs

Yanbo Jia and David Cebon

**Abstract**—This paper focuses on measuring the motion of a cyclist moving adjacent to a heavy goods vehicle (HGV), from the detections of ultrasonic sensors installed along the side of the vehicle. The measurements are used in a prototype collision avoidance system that predicts the future relative motion and assesses the likelihood of a collision. An array of ultrasonic sensors is adopted to cover the near side of the HGV, where most of fatal collisions with cyclists occur. A method combining quadratic programming and Kalman filtering is developed in this paper for recovering the bearing angles of the cyclist from the detected distances provided by off-the-shelf ultrasonic sensors. The algorithms are developed for use in real time and practical constraints are considered. The simulation and testing results prove the effectiveness of the proposed method for a reasonable range of the speed differential between the cyclist and the HGV.

**Index Terms**—collision avoidance, heavy goods vehicles, motion estimation, quadratic programming, ultrasonic sensors, vulnerable road users

## I. INTRODUCTION

HGVs are a major contributing factor for accidents involving cyclists, especially those resulted in fatalities. Between 2009 and 2013 they were involved in around a quarter of cyclist deaths in the UK [1].

Transportation Research Laboratory (TRL) investigated HGV-related accidents between 2006 and 2008. They reported that on average, HGVs cause 27 deaths and 72 serious injuries to cyclists each year in the UK. Among these, side-to-side collisions account for 43% of fatalities and 36% of serious injuries to cyclists [2]. In recent years, research and commercial systems have started focusing on collision prevention for cyclists and pedestrians, based on either camera only ([3] [4] [5]) or sensor fusion of camera and radar [6].

Existing technologies have also looked into protecting cyclists on the nearside of heavy vehicles, by:

- (i) providing the driver with side-view cameras, 360° view cameras [7], or simply more wing mirrors [8] for better visibility of blind spots;
- (ii) utilising ultrasonic sensors on the side of the vehicle to

detect cyclists who are in close proximity;

- (iii) use of radar based technology [9] for cyclist monitoring.

A collision avoidance strategy was introduced in [10] and [11], aimed at estimating the motion of the cyclist relative to the truck and intervening in the truck's motion when a collision is predicted. The methods of collision prediction is detailed in [10]. There are a variety of sensing methods for detecting objects around a vehicle (summarized in [11]), including camera, radar, lidar and ultrasonic sensors. Ultrasonic sensors were selected in this study because:

- 1) The characteristics of the detection geometry are well suited to ultrasonic sensors. The lateral distance from the cyclist to the HGV is normally less than 2m, which matches the detection range of a typical ultrasonic sensor.
- 2) Ultrasonic sensors can provide distance measurements of acceptable accuracy (5mm of error can be achieved);
- 3) Ultrasonic sensors can work in a variety of weather conditions (including fog, rain, low and high temperatures, etc) and any light levels;
- 4) The low cost of ultrasonic sensors makes them commercially attractive.

An ultrasonic sensor suitable for detecting humans has a beam width typically less than 2m, which is significantly less than the length of a typical lorry (>10m). So it is necessary to deploy multiple sensors to cover the near side of an HGV.

Ultrasonic sensors have been used in various applications in recent years. In [12] the authors describe spatial reconstruction of orthogonal planes using a rotary array of ultrasonic sensors. In [13], 24 ultrasonic sensors were used, spaced with an angular displacement of 15° and mounted on top of the robot, to achieve navigation of autonomous mobile systems. Multiple sensors are also used for improving accuracy in distance measurement [14] and [15]. For parking assistance on automobiles, four sensors are often deployed to locate objects by triangulation [16]. None of these research or commercial systems tracks the motion of the objects they detect.

An array of multiple ultrasonic sensors is also akin to the layout of SONAR sensors ('multi-beam echo sounders') used in 'bathymetry' and underwater navigation. With SONAR, target positioning relies on beamforming (or beam steering), which require processing raw reflected waves [17]. The sensors are used to scan a line across the sea floor underneath a towing

Paper submitted for review on 25th July, 2017.

Yanbo Jia, PhD, is with Department of Engineering, University of Cambridge, Trumpington Street, Cambridge CB2 1PZ, UK (email: yj253@cam.ac.uk).

David Cebon, Prof., BE, PhD, FREng, FIMechE, is with Department of Engineering, University of Cambridge, Trumpington Street, Cambridge CB2 1PZ, UK (e-mail: dc@eng.cam.ac.uk)

Corresponding author: David Cebon (email: dc@eng.cam.ac.uk).

vessel and the data is used to map the topography (depth) of the sea-floor.

Given the distance to the target measured by ultrasonic sensors, it is not possible to pinpoint the exact position of a target because the bearing angle from the sensor to the target is unknown. The position of a target alongside a vehicle could be anywhere on the arc with the same radius as shown in Fig. 1. This is termed 'position ambiguity'. To construct the cyclist's motion relative to the truck, it is necessary to recover the bearing information (Fig. 2). This paper discusses a novel approach for bearing angle estimation, purely based on the detected distances from ultrasonic sensors. The approach discussed in this paper is designed for cyclist motion estimation and tracking for a collision avoidance system ([10] and [11]) whose focus is to prevent side-to-side collisions between HGVs and cyclists.

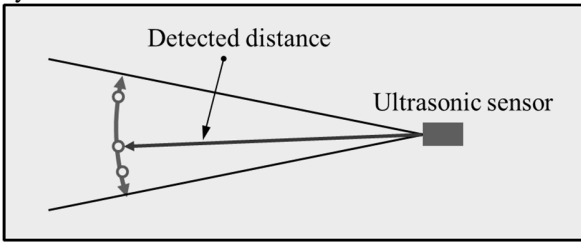


Fig. 1 Illustration of position ambiguity by ultrasonic sensor detection

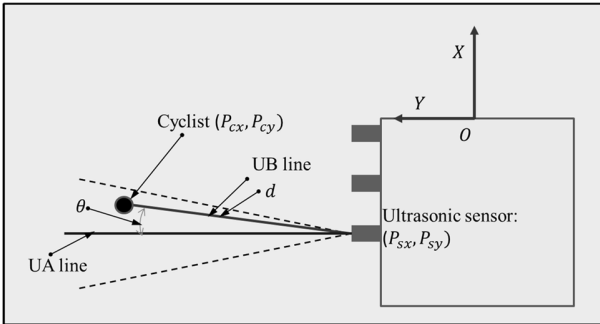


Fig. 2 Illustration of the bearing angle for the ultrasonic sensor detection

Ultrasonic sensors are installed at the cyclist's shoulder height on the HGV [10]. This allows the sensors to capture a narrow side profile of the cyclist bicycle combination, eliminating the risk of detections being from different parts of the bicycle and cyclist. The detections are always consistent and the whole problem can be simplified to that of estimating the location and motion of a point mass and then extrapolating to the combination of the rider and the bicycle. The field testing of the system described in [11] has proved the effectiveness of this methodology.

The methods proposed in this paper are concerned with object localisation. They are not in the same category as the computer vision based methods, such as [18], [19], [20], [21], [22] and [23], which are generally concerned with front-end collision warnings or traffic monitoring from roadside cameras. Nor are they related to wave based methods for radar [24] and sonar [17], which are concerned with bearing calculations and are not cyclist detection. The approach described in this paper is unique. The combination of an array of multiple, high-performance ultrasonic sensors, processed using Quadratic

Programming and Kalman Filtering, provides an accurate measurement of (past and) current position of the cyclist and a prediction of future relative motion. This was not previously possible.

## II. POSITION ESTIMATION ALGORITHM

### A. Overview of the Propose Algorithms

Fig. 3 is a schematic diagram of the overall algorithm for cyclist position information. It shows how the positions of the cyclist can be estimated in real time, based on detected distances from ultrasonic sensors. Each ultrasonic sensor outputs the measured distances with its sensor ID. This information is first sent to a processor that checks if there are any possible triangulations formed between neighbouring sensor detections (discussed in more detail in the next section). As there can be multiple detections at each time step, a process called 'ID sequencing' is introduced to help discount spurious sensor detections that are irrelevant to the motion of a cyclist. An optimization algorithm using a quadratic programming (QP) approach is used to determine the best set of detection angles  $\theta$  and the corresponding positions of the cyclist. A Kalman filter is then used to smooth the trajectory of the cyclist based on a kinematic model of the cyclist's relative motion. The steps are detailed below.

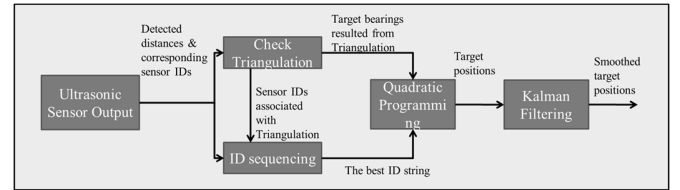


Fig. 3 Schematic for position estimation in real time

### B. Triangulation

If two neighbouring ultrasonic sensors  $US_k$  and  $US_{k+1}$  have overlapping detection ranges and the cyclist falls into the overlap area, there will be two detected distances  $d_k$  and  $d_{k+1}$  available to process at the same time in the data stream, as shown in Fig. 4. Two sensors and the target form a triangle, and it is straightforward to find out each angle inside the triangle by applying cosine rules. It is not necessarily true that any two detections from neighbouring sensors at the same time could form a triangulation. The detailed methods for forming triangulations are described in [11]. Once a triangulation is found, it is necessary to check whether the calculated bearings are valid or not by comparing them with the maximum angle that forms the field of view of the sensors. The bearings resulting from triangulations can be used to provide 'equality constraints' in the Quadratic Programming step (see later).

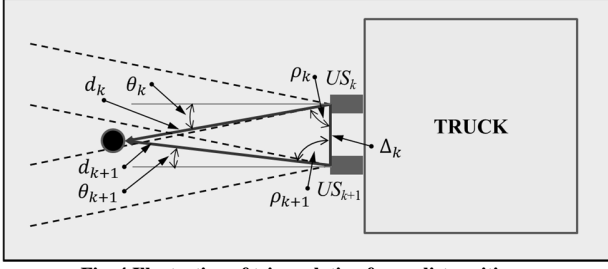


Fig. 4 Illustration of triangulation for cyclist position

### C. Sensor ID Sequencing

It is important to associate detected distances with specific objects correctly. This is termed as ‘data association’ in object tracking tasks. The purpose of this paper is to illustrate a new method for motion estimation only; therefore, data association methods will not be used. Instead it is assumed that only one object is in view of the sensor system at any time. Estimating the motion of multiple cyclists moving in an array of ultrasonic sensors is the subject of ongoing work.

For the case where only one object of interest is concerned, it is also possible that there is more than one detection at a time, due to (i) ultrasonic reflections from neighbouring sensors; (ii) environmental noise and random reflections or sensor errors. This problem can be compounded by occasional spurious detections from noisy sensors. As a result, it was found necessary to eliminate sensor detections that prevented the forming of a smooth cyclist trajectory.

A heuristic method of ID sequencing for one object of interest is detailed in [11]. In summary, the output of the ID sequencing step is a string of sensor IDs, with each element corresponding to a time step during the period to inspect (PTI) chronologically. All possible ID combinations are generated for the PTI and for all these combinations, the differences between elements in each combination are calculated. These differences indicate the motion ‘trend’ of the cyclist. If they are positive, the cyclist is moving forwards relative to the truck; if they are negative, the cyclist is moving backwards.

If valid triangulations are found during the PTI, the associated sensor IDs with shorter detected distances in each triangulation pair are used as ID ‘boundaries’ that divide the full ID string into several sections. In each ID section, the same rules for sequencing IDs are applied, i.e.:

- 1) ID discontinuities are not allowed;
- 2) non-monotonic ID sections are not allowed;
- 3) IDs associated with outliers are ignored.

### D. Problem formulation of position estimation

It is assumed that an array of ultrasonic sensors is installed on the nearside of HGV to cover the entire lateral side of the truck. The front sensor is assigned with ID number 1, while the rear sensor has number N. The choice of N depends on vehicle length and sensor spacing.

A coordinate system defines the positions of ultrasonic sensors on the truck as well as the cyclist’s position. The origin

is set at the mid-point on the front edge of the vehicle, with  $x$  axis along the longitudinal direction and  $y$  axis pointing to the left of the vehicle (shown in Fig. 2).

A reference line (UA) is defined for each sensor, pointing along the outwards normal to the side of the vehicle. The line from the sensor to the target is a position vector. The angle from the reference line to the position vector is defined as the target bearing  $\theta$ . Clockwise rotation of  $\theta$  is defined as positive.

Given the lateral and longitudinal positions of one ultrasonic sensor ( $P_{sx}, P_{sy}$ ) in this coordinate system and the detected distance  $d$ , the cyclist position ( $P_{cx}, P_{cy}$ ) relative to the HGV can be expressed by the following equations:

$$P_{cx} = P_{sx} + d \cdot \sin\theta \quad (1)$$

$$P_{cy} = P_{sy} + d \cdot \cos\theta \quad (2)$$

On the right hand side of both equations (1) and (2), the only unknown parameter is  $\theta$ . Therefore, the problem essentially becomes to choose a value for  $\theta$  given the detected distance and sensor positions on the truck.

### E. Quadratic Programming

#### 1) Equation formulation

It is not possible to solve (1) and (2) independently, as the number of equations is smaller than the number of unknowns, rendering the equations indeterminate mathematically. For a single object, given a series of detected distances ( $d_1, d_2, d_3, \dots, d_n$ ) for a short period of time ( $t_1, t_2, \dots, t_n$ ), it is necessary to find out the corresponding bearings ( $\theta_1, \theta_2, \dots, \theta_n$ ) so that the longitudinal positions ( $P_{cx,1}, P_{cx,2}, P_{cx,3}, \dots, P_{cx,n}$ ) and lateral positions ( $P_{cy,1}, P_{cy,2}, P_{cy,3}, \dots, P_{cy,n}$ ) can be determined; i.e. the following equations must be solved:

$$P_{cy,i} = P_{sy,i} + d_i \cdot \cos\theta_i \quad (3)$$

$$P_{cx,i} = P_{sx,i} + d_i \cdot \sin\theta_i \quad (4)$$

where  $i=2,3,\dots,n$ .

Using simple numerical differentiation, the cyclist’s velocity  $V$  and the acceleration  $A$  relative to the HGV can be obtained, as follows:

$$V_{cx,j} = \frac{(P_{cx,j} - P_{cx,j-1})}{(t_j - t_{j-1})} \quad (5)$$

$$V_{cy,j} = \frac{(P_{cy,j} - P_{cy,j-1})}{(t_j - t_{j-1})} \quad (6)$$

$$A_{cx,l} = \frac{(V_{cx,l} - V_{cx,l-1})}{(t_l - t_{l-1})} \quad (7)$$

$$A_{cy,l} = \frac{(V_{cy,l} - V_{cy,l-1})}{(t_l - t_{l-1})} \quad (8)$$

where  $j=2,3,\dots,n$ ; and  $l=3,4,\dots,n$  and  $t$  is the time stamp for each detection. Given  $n$  samples,  $n-2$  lateral and longitudinal acceleration terms, can be obtained from (7) and (8).

It is worth highlighting that the subscripts  $i, j$  and  $l$  represent instances for detections over a contiguous period of time, and

these detections can be from one single sensor or several sensors, depending on the relative speed between the object and the truck. It is important not to misread these subscripts as sensor ID numbers.

Combining equations (5) and (7), the longitudinal acceleration  $A_{cx,l}$  at the  $l$ th's step of the object can be expressed as:

$$A_{cx,l} = W_{1,l} * \sin\theta_{l-2} + W_{2,l} * \sin\theta_{l-1} + W_{3,l} * \sin\theta_l + W_{4,l} \quad (9)$$

Where  $l=3,4 \dots, n$ ,  $W$  represents the coefficients whose detailed expressions are provided below.

$$W_{1,l} = \frac{d_{l-2}}{(t_{l-1} - t_{l-2}) \cdot (t_l - t_{l-1})} \quad (10)$$

$$W_{2,l} = \frac{-(t_l - t_{l-2}) \cdot d_{(l-1)}}{(t_{l-1} - t_{l-2}) \cdot (t_l - t_{l-1})^2} \quad (11)$$

$$W_{3,l} = \frac{d_l}{(t_l - t_{l-1})^2} \quad (12)$$

$$W_{4,l} = \frac{(t_{l-1} - t_{l-2}) \cdot P_{sx,l}}{(t_{l-1} - t_{l-2}) \cdot (t_l - t_{l-1})^2} - \frac{(t_l - t_{l-2}) \cdot P_{sx,l-1}}{(t_{l-1} - t_{l-2}) \cdot (t_l - t_{l-1})^2} + \frac{(t_l - t_{l-1}) \cdot P_{sx,l-2}}{(t_{l-1} - t_{l-2}) \cdot (t_l - t_{l-1})^2} \quad (13)$$

For each acceleration term  $A_{cx,l}$ , the only unknowns are  $\sin\theta_{l-2}$ ,  $\sin\theta_{l-1}$ , and  $\sin\theta_l$ . Treating  $\sin\theta$  as a whole, the expression of  $A_{cx,l}$  can then be seen as a summation of three linear terms.  $\cos\theta_l$  can be obtained once  $\sin\theta_l$  is determined. Consequently, the positions  $P_{cx,l}$  and  $P_{cy,l}$  can be found.

## 2) Objective Function

It is hypothesised that the best set of  $\theta$  values in the time span PTI are the ones that yield the smoothest longitudinal acceleration profile. These are found by finding the set of  $\theta$  values that minimize the objective function:

$$J = \sum_{l=3}^n (A_{cx,l} - \bar{A}_{cx})^2 \quad (14)$$

where,  $\bar{A}_{cx}$  is the average longitudinal acceleration of the cyclist during the PTI. The objective in (14) indicates that the minimum of  $J$  can be achieved when  $A_{cx,l}$  equals  $\bar{A}_{cx}$ , which is an unknown parameter at the start of the optimization as we have no *a priori* knowledge of the cyclist motion.

Expanding (14) in polynomial form and treating  $\bar{A}_{cx}$  as a coefficient, this equation can be rewritten as:

$$J = \sum_{l=3}^n (A_{cx,l})^2 - 2 \cdot \bar{A}_{cx} \cdot \left( \sum_{l=3}^n A_{cx,l} \right) + (n-3) \bar{A}_{cx}^2 \quad (15)$$

The term  $(n-3) \bar{A}_{cx}^2$  in (15) does not contain any bearings and therefore does not affect the optimization results and can be neglected. The term  $2 \cdot \bar{A}_{cx} \cdot (\sum_{l=3}^n A_{cx,l})$  contains linear functions of the bearing angles.

Each acceleration term  $A_{cx,l}$  can be expressed in a function of bearing angles ( $\sin\theta_{l-2}, \sin\theta_{l-1}, \sin\theta_l$ ) as shown in Equation (9). Replacing  $A_{cx,l}$  by  $\sin\theta_l$  and defining  $\Theta = [\sin\theta_1, \sin\theta_2, \dots, \sin\theta_n]^T$  (superscript T means transpose), the objective function can be rewritten in quadratic form:

$$f(\Theta) = \frac{1}{2} \Theta^T Q \Theta + L \Theta \quad (16)$$

where  $Q$  is an  $n$  by  $n$  matrix and is called the quadratic matrix, and  $L$  is a  $n$ -variable row vector and is called the linear matrix.

This cost function can be minimized subject to sets of 'equality' and 'inequality' constraints, using one of the standard 'quadratic programming' (QP) methods [25]. The equality constraints are defined by:

$$A_{eq} \Theta = B_{eq} \quad (17)$$

while the inequality constraints are:

$$A_{in} \Theta \leq C_{in} \quad (18)$$

Equality constraints provide strict limits on some of the variables in  $\Theta$  and thus enable more accurate optimization results. These are derived from possible triangulations found in the sensor outputs. In constructing matrices  $A_{eq}$  and  $B_{eq}$ , the number of inequality constraints should not be equal or greater than the number of variables in  $\Theta$ , otherwise the problem is over-constrained and QP cannot converge to a solution.

The inequality constraints in (18) are associated with two types of conditions: angle limits and motion limits. For angle limits, each element in  $\Theta$  must be limited to its own upper and lower boundaries which come from the expected width of the sensor beams. For motion limits, elements in  $\Theta$  should follow a trend that conforms to the motion of the object relative to sensor. If the cyclist overtakes the truck, the bearing associated with each sensor changes from  $-ve$  to  $+ve$  in each sensor's detection range, and vice versa when the truck is overtaking the cyclist. If the cyclist stays in one sensor's range for a short period of time, it is necessary to be consistent with the motion trend deduced from previous step

If no *prior* knowledge about cyclist's motion is available, it is safe to assume that the cyclist is travelling at a similar speed to the truck. In this case, it's impossible to pose motion constraints other than upper and lower bounds.

It is possible to estimate the relative yaw angle, based on the trajectory of the cyclist and this is used in [11] to predict the future position of the bicycle. For the collision scenarios that we are trying to measure, the yaw angle between cyclist and lorry is relatively small. If the angle is large, the approach velocity is likely to be high and a collision is inevitable.

For the objective function (14) under constant acceleration assumption,  $\Theta$  can only be solved when the value of  $\bar{A}_{cx}$  is known. In practice  $\bar{A}_{cx}$  is inherited from previous steps. When no previous knowledge of  $\bar{A}_{cx}$  is available, it is estimated using an iterative method that takes guesses for  $\bar{A}_{cx}$ . An initial

estimate for  $\bar{A}_{cx}$  is made by selecting values in the range from  $-2\text{m/s}^2$  to  $2\text{m/s}^2$  with a resolution of  $0.1\text{m/s}^2$ . With each sample for  $\bar{A}_{cx}$ , a candidate for  $\Theta$  can be derived using QP. Each candidate for  $\Theta$  is passed to (3) and (4) to get the cyclist positions for the PTI and the accelerations using (5) to (8). The standard deviation of the lateral accelerations is calculated.

After running through all the candidates for  $\Theta$ , a series of standard deviations is obtained. Comparing these standard deviations, the smallest deviation is chosen and the corresponding  $\Theta$  is then selected as the best estimation for cyclist bearings. The sample for  $\bar{A}_{cx}$  that produces  $\Theta$  is believed to be the best estimation for the acceleration during the PTI. It is possible that this calculation can be streamlined to reduce the computation time.

Another possible assumption is constant longitudinal velocity for the object during PTI, in which case,  $\bar{A}_{cx}$  is changed to 0 and the objective function  $J$  (14) becomes.

$$J = \sum_{l=3}^n A_{cx,l}^2 \quad (19)$$

The standard quadratic form of this function contains the same  $Q$  term but different  $L$  term. The constraints (17) and (18) still hold.

The resulting  $\sin\theta_n$  corresponds to the most recent detection and can be used in real time to derived the cyclist's current location based on Equation (3) and (4).

#### F. Kalman Filtering for Position Estimation

In practice, there are some inaccurate detections (ultrasonic pings are not always reflected from the same point of the cyclist) and signal dropouts. It is therefore difficult to obtain a smooth trajectory for the cyclist purely based on quadratic programming.

Further smoothing is needed to produce a trajectory from which velocities and accelerations can be derived – and used for estimating the future motion. A Kalman filter was selected to smooth the output of QP process. Kalman filters are widely used in guidance, navigation and control systems for vehicles, as well as motion tracking [26]. Using a model of the system, a Kalman filter can smooth a time series of measurements, containing noise and other inaccuracies.

The cyclist's motion can be described purely in terms of its kinematics. The state vector expressing the kinematics is coined as  $S$  and it is constructed by cyclist's positions and velocities in both longitudinal and lateral directions:

$$S = [P_{cx}, P_{cy}, V_{cx}, V_{cy}]^T \quad (20)$$

The state space equation for Kalman filter can be written as:

$$S_{l+1} = A_{kf} \cdot S_l + B_{kf} \cdot U_{l+1} + w_l \quad (21)$$

$$A_{kf} = \begin{bmatrix} 1 & 0 & dt & 0 \\ 0 & 1 & 0 & dt \\ 0 & 0 & 1 & 0 \\ 0 & 0 & 0 & 1 \end{bmatrix}$$

$$B_{kf} = \begin{bmatrix} \frac{1}{2} dt^2 & \frac{1}{2} dt^2 & dt & dt \end{bmatrix}^T$$

The 'control input'  $U$  is the cyclist acceleration, and  $w$  represents Gaussian white noise in the process. This noise is assumed to have zero mean and a variance matrix defined as  $G$ .

$$G = \begin{bmatrix} \frac{\Delta t^4}{4} & 0 & \frac{\Delta t^3}{2} & 0 \\ 0 & \frac{\Delta t^4}{4} & 0 & \frac{\Delta t^3}{2} \\ \frac{\Delta t^3}{2} & 0 & \Delta t^2 & 0 \\ 0 & \frac{\Delta t^3}{2} & 0 & \Delta t^2 \end{bmatrix} \cdot \sigma_a^2 \quad (22)$$

The measurement equation is expressed as:

$$H_{l+1} = C_{kf} \cdot S_l + v_l \quad (23)$$

$$C_{kf} = \begin{bmatrix} 1 & 0 & 0 & 0 \\ 0 & 1 & 0 & 0 \end{bmatrix}$$

with  $H$  being the output vector, and  $v$  being the measurement noise, which is also of Gaussian white distribution, and its covariance matrix is denoted as  $R$ .

$$R = \begin{bmatrix} \sigma_x^2 & 0 \\ 0 & \sigma_y^2 \end{bmatrix} \quad (24)$$

The Kalman filter works in two stages: time update and measurement update [26]. Time update, also known as prediction, is for predicting values of the current state variables and error covariance estimates, to obtain the *a priori* estimates for the next time step. The following two equations are called time update equations, with  $Z$  being the model covariance matrix:

$$\hat{S}_{l+1}^- = A_{kf} \cdot \hat{S}_l + B_{kf} \cdot \hat{U}_l \quad (25)$$

$$Z_{l+1}^- = A_{kf} \cdot Z_{l+1} \cdot A_{kf}^T + G_l \quad (26)$$

The '^' indicates that the derived value is an estimate, and the superscript '-' means an *a priori* estimate. The measurement update equations incorporate a new measurement into the *a priori* estimate to obtain an improved *a posteriori* estimate.

Once new measurements are available, these estimates are updated based on a weighted average of the estimates and measurements, with more weighting being assigned to estimates with higher certainty.

In the measurement update stage, the Kalman gain  $K$  is updated using (27). With the updated Kalman gain, the state  $S$  is recalculated considering measurement  $H$  in (28). The covariance matrix  $Z$  is further updated in the meantime, as per (29).

$$K_{l+1} = Z_{l+1}^- \cdot C_{kf}^T (C_{kf} \cdot Z_{l+1}^- \cdot C_{kf}^T + R)^{-1} \quad (27)$$

$$\hat{S}_{l+1} = \hat{S}_{l+1}^- + K_{l+1} \cdot [H_{l+1} - C_{kf} \cdot \hat{S}_{l+1}^-] \quad (28)$$

$$Z_{l+1} = (I - K_{l+1} \cdot C_{kf}) Z_{l+1}^- \quad (29)$$

The variable  $I$  in (29) is a 4 by 4 identity matrix.

Equations (25) to (29) are the core equations in a Kalman filter which can be run recursively to find the best estimate of the state vector. In this study, it was found reasonable to assume  $U_l$  is 0, because the experimental tests were performed at essentially constant relative velocities. However, this assumption needs to be verified for a wider range of conditions.

To start the Kalman filter, the initial state is estimated as a column vector with 4 zero elements and the initial value of covariance matrix  $Z$  is set as  $G$ . The algorithm is recursive and therefore is suitable for real time application.

### III. SIMULATION RESULTS

#### A. Constant velocity simulations

A simple simulation model was set up to test the QP approach for deducing a cyclist's trajectory from knowledge of the detected distances. A sensor spacing of 0.8m was defined in the model and a triangular range was assumed for each sensor in the simulation. This shape defined the upper and lower limits for the target bearing angle. The sampling rate was initially fixed at 7.5Hz to match the outputs of commercially available sensors. Various constant relative velocities were simulated, ranging from -15 to 15 km/h. A negative relative speed indicates that the truck overtakes the cyclist. Several cyclist manoeuvres were tested in the model. These were:

- 1) Cyclist travelling parallel to the truck, with a lateral spacing of 1.2m, moving from the rear end towards the front of the truck;
- 2) Cyclist travelling diagonally, starting at 1.2m away from the truck laterally, from the rear end and closing towards the front end;
- 3) Cyclist travelling diagonally, starting at 1.2m away from the truck laterally, from the front end and closing towards the rear end.

##### 1) Parallel Motion

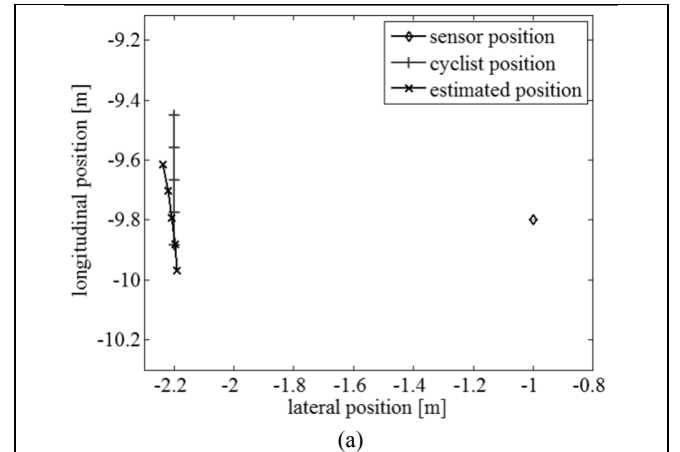
For the parallel motion tests, the relative speed of the cyclist was set as 3km/h. Fig. 5 shows the results of the quadratic programming step for five outputs from a single sensor. Fig. 5(a) shows the estimated positions of the cyclist compared with its true simulated positions. The positions of the sensors that are associated with these samples are plotted as well. Fig. 5(b) shows estimated and true target bearings relative to the sensor.

During the time span when 5 samples are collected (Fig. 5(a)), the detected distances are all from the same sensor. In this case,

the deviation of the estimated positions from the true positions is relatively large because the objective function is not strictly convex and the optimization stops when a local minimum is found for the objective function. These local minima may not be the desired solutions. Two or more sets of bearings could lead to the same minimum value of the objective for the same dataset. When the sample number is increased to 10 and two sensors are involved, the estimation is significantly improved, as shown in Fig. 6(a). The bearing angles increase up to  $18^\circ$  as the cyclist passes the first sensor (Fig. 6(b)), from 0.3 to 0.9s. The reading at 1.1s comes from the second sensor, so the bearing angle 'flies back' to  $-17^\circ$ , then increases as the cyclist passes the second sensor. The agreement between the 'true' and estimated values of the bearings is good.

Fig. 7 is for the same manoeuvre as described in Fig. 5 and Fig. 6, but showing just the bearing angles. Fig. 7(a) is for the case where the sample size is 15 and Fig. 7(b) is for size 20. These two graphs show a similar pattern of accuracy for the estimated positions. When more sensors are involved in the QP, the estimated positions almost overlap the true positions. Given that the sampling rate is fixed, when more sensors are involved in the QP, more samples are needed.

Conversely, more samples require a longer calculation time, which is less favourable because less time is available for predicting and avoiding potential collisions. A larger sample set for QP can also lead to a greater computational overhead, as the size of the matrices increase (especially for generating all of the ID combinations in the ID sequencing stage). 15 samples in the PTI are selected for a good accuracy, yet efficient computation for real time estimation.



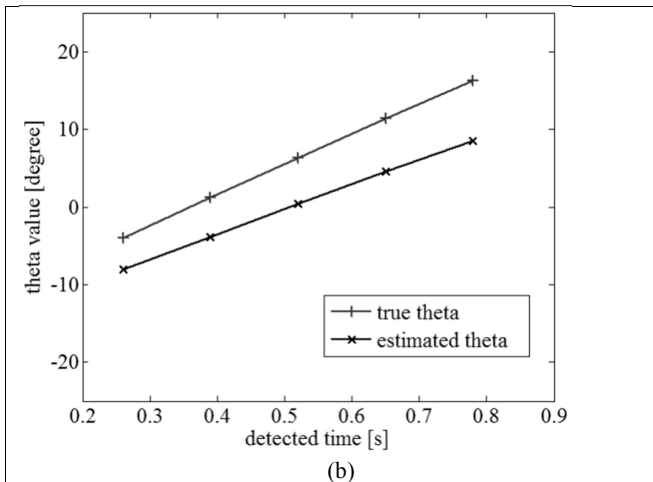


Fig. 5 Output of Quadratic Programming calculation for five sample points from one sensor, assuming constant relative velocity. (a), Positions of the sensor and cyclist. (b) Estimated values of  $\theta$

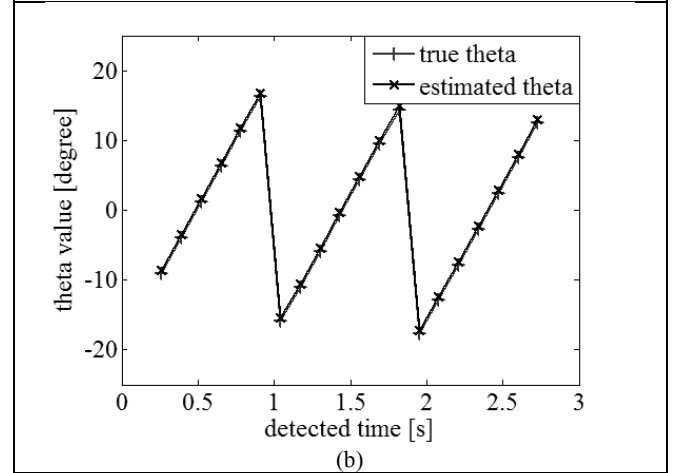
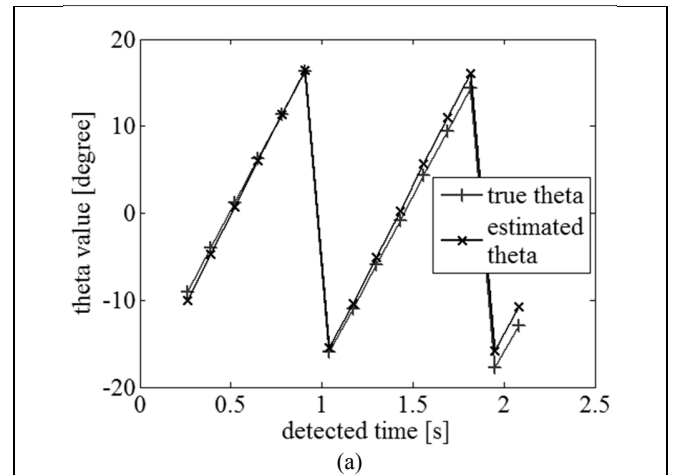


Fig. 7 Comparison of different sample set sizes for the quadratic programming

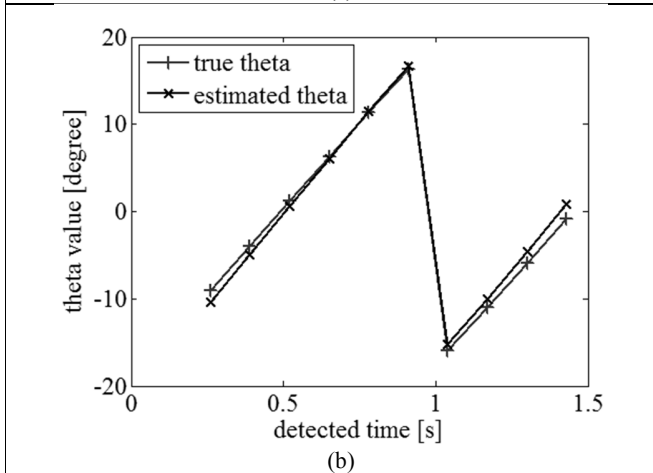
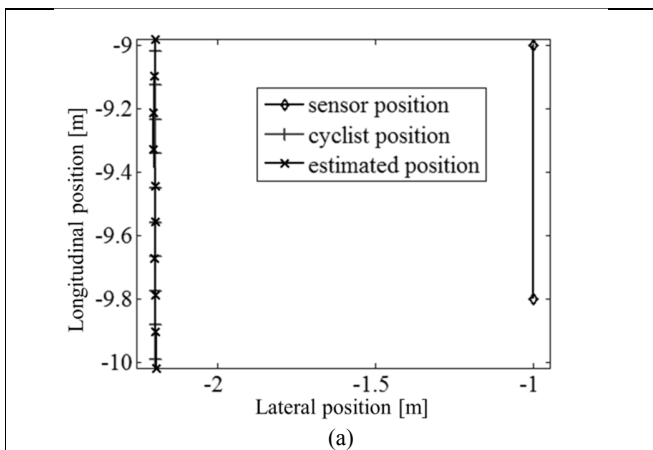


Fig. 6 Output of Quadratic Programming calculation for ten sample points from two sensors, assuming constant relative velocity. (a), Positions of the sensor and cyclist. (b) Estimated values of  $\theta$

## 2) Converging and Diverging Motion

The QP should be able to calculate the cyclist's trajectory no matter what the motion of the cyclist relative to the truck. The simulation results shown in Fig. 8 are for a manoeuvre where the cyclist moves at an angle relative to the truck. Fig. 8(a) illustrates the case when the cyclist moves from the rear end of the truck to the front, while steering away from the truck. In Fig. 8(c), the cyclist moves from the front end of the truck to the rear. This equates to a manoeuvre where the truck overtakes the cyclist. The lateral distance between the two increases as the manoeuvre progresses. Both figures show that the estimated positions of the cyclist match the true positions accurately. Fig. 8(b) and (d) show that the bearing angles are estimated accurately by the QP process.

Both a faster sampling rate and a larger number of samples improve the accuracy of the QP algorithm. In practice, the sampling rate depends solely on the type of ultrasonic sensors. In a real-time system, the number of samples in each QP calculation needs to be kept constant because this number determines the sizes of most of matrices in the calculation. Given that both the sampling rate and the number of samples are essentially fixed, it is of interest to understand how the relative speed of the motion between the cyclist and the truck

affects the performance of the optimization.

To evaluate the performance of the QP across a range of relative speeds, the bearing associated with each sample was compared with the true bearing. The maximum, average and minimum value of the bearing errors for all the samples at each run of the QP were recorded. These values are plotted for relative speeds ranging from -15 km/h to 15 km/h in Fig. 9 with the sample size in each QP calculation being fixed at 15. In the figure, the three '+' signs in each vertical line are the maximum positive, average, and maximum negative bearing errors respectively.

It is noticeable that QP produces large estimation error when the relative speed is zero. If the cyclist stays in one sensor's detection range for the PTI and the detected distance doesn't change, QP fails to estimate the relative motion of the cyclist correctly. However, this scenario is regarded as safe because that there is no relative motion between the cyclist and the truck.

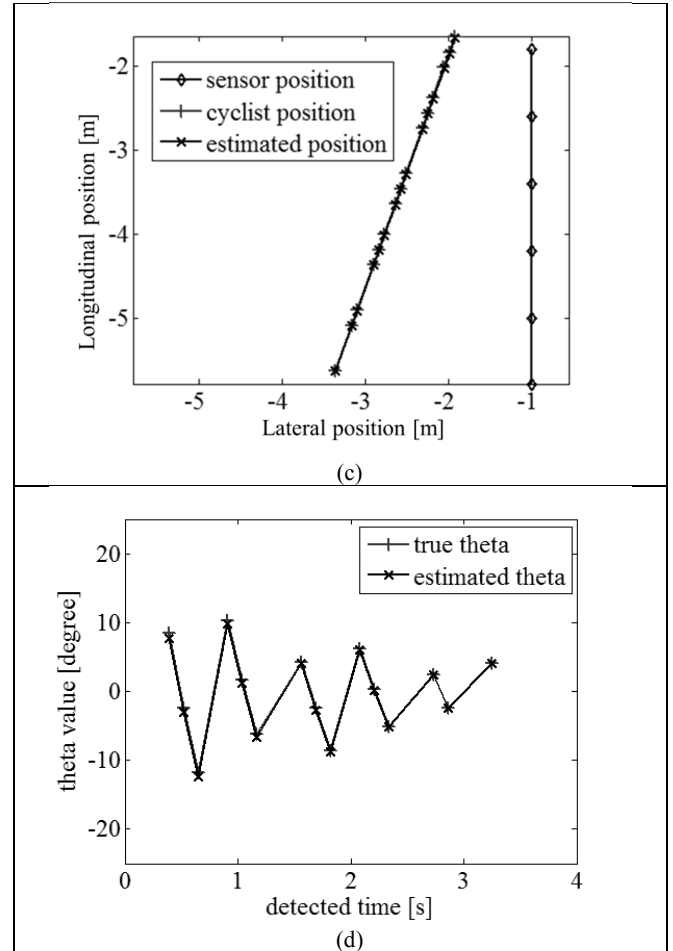
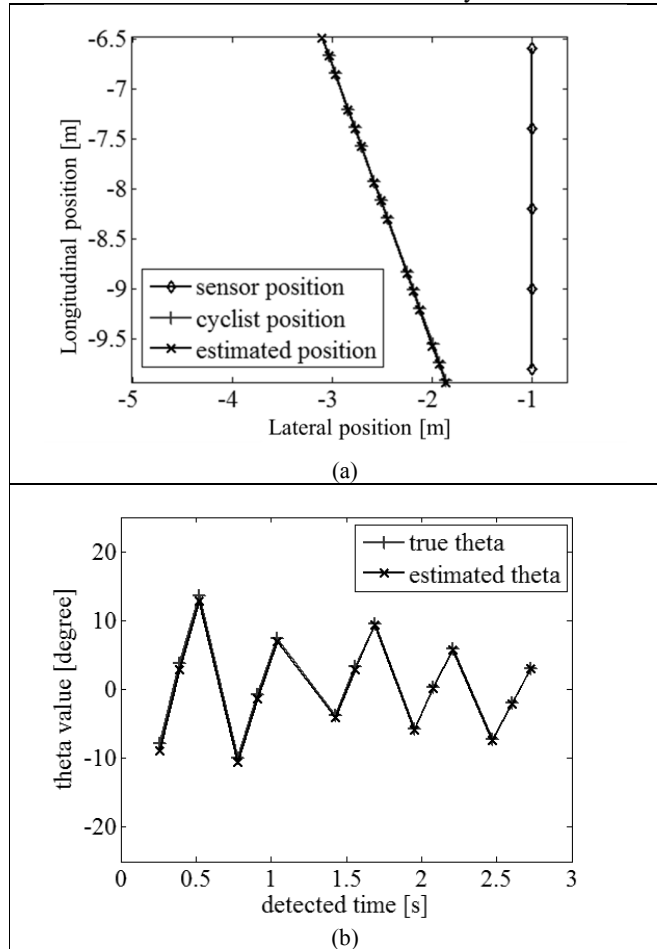
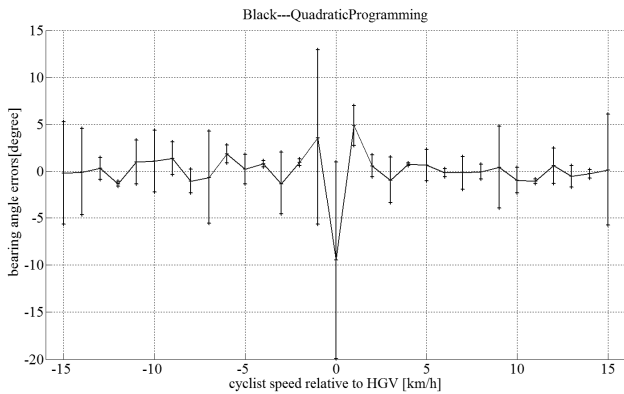


Fig. 8 Comparison of diagonal manoeuvres: (a) cyclist steers away from the truck on the front side; (b) estimated cyclist bearings for the manoeuvre in (a); (c) equal to truck overtakes the cyclist and steers away from the cyclist; (d) estimated cyclist bearings for the manoeuvre in (c)

Fig. 9 shows that the mean error is close to zero and essentially independent of the relative speed. There are some speeds where the errors are very small, and some where they are larger. This variation is a result of interaction between the sampling time, the speed, the start position of the cyclist and the field of view of the sensors.

Comparisons for different sample sizes were conducted in [11] and it was concluded that higher sample sizes can offer better optimization results, but there is no benefit of increasing the sample size above 15 for these test conditions.



**Fig. 9 Comparison of absolute bearing errors for different relative speed between the cyclist and the HGV**

### B. Constant acceleration assumption for quadratic programming

This section investigates the efficacy of the constant acceleration approach. In the simulations, the cyclist was assigned a relative longitudinal acceleration of  $1\text{m/s}^2$  for the relative speed range of  $1\text{km/h}$  to  $15\text{km/h}$  and  $-1\text{m/s}^2$  for the range of  $-1\text{km/h}$  to  $-15\text{km/h}$ . The cyclist started from the rear end of the truck for the case with a positive relative speed, and the front end for a negative relative speed. A parallel manoeuvre was used with the lateral distance being  $1.2\text{m}$ . The sampling rate was  $7.5\text{Hz}$  and the size of the sample set was 15. Both versions of the QP calculation were used: constant velocity and constant acceleration.

Fig. 10 offers some comparisons between the bearings resulted from the QPs with both constant velocity model and constant acceleration model for a relative speed at  $6\text{km/h}$ . It can be seen that the model with constant acceleration works better for the QP than the constant velocity model when there is no knowledge of the acceleration of the cyclist. Very similar results were found for simulations at other relative speeds [11].

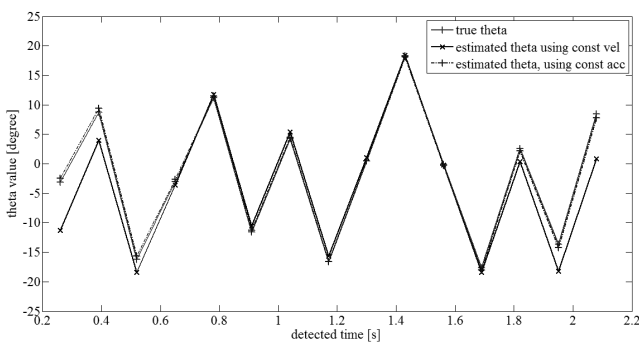


**Fig. 10 Comparison of the bearings using the two QP models with a relative speed of  $6\text{km/h}$ .**

The estimated accelerations for each relative speed are plotted in Fig. 11. The maximum absolute acceleration error is  $0.2\text{m/s}^2$  while a majority of the estimated accelerations match the 'true' values. For instance, at a relative speed of  $3\text{km/h}$ , the acceleration error is  $-0.1\text{m/s}^2$ . The scale of the error also depends on the resolution of the acceleration sample set: a finer resolution would produce an estimate of the acceleration closer

to the true value; however, it would add significantly to the computational time because more runs of QP would be needed.

It can be concluded that the results are not perfectly accurate, but are still good enough for estimating the longitudinal acceleration and significantly more accurate than using constant velocity model in constructing the QP equations.

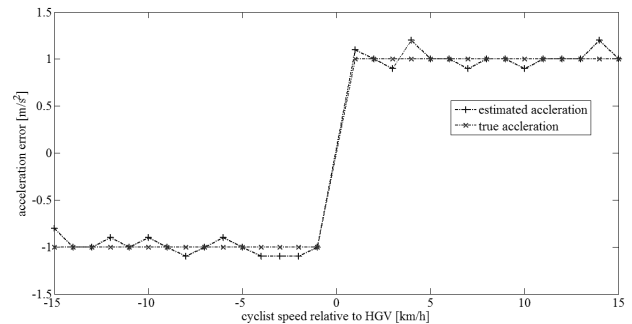


**Fig. 11 Estimation results using QP only and QP with Kalman filter, cyclist  $5\text{kph}$  faster than the HGV, cyclist parallel to HGV**

### C. Optimization Results for QP and Kalman Filtering

In practice, the ultrasonic sensors use the strongest reflection from the cyclist to form successful registrations. The ultrasonic waves reflected to the sensor are not always from the same point on the side of the cyclist, because the closest point from the cyclist to the sensor varies depending on the cyclist's posture and relative positions. So the detected distances registered by the ultrasonic sensors are likely to be noisy.

At each time step, the QP optimization is run for the PTI which includes a fixed number of samples, with the last sample being the latest detection. The cyclist positions in the PTI are deduced accordingly. On the next time step, the sample set is updated by including the newest detected distance and removing the oldest data. The QP is conducted for the new series of cyclist positions in the current PTI. In the real-time process, only the last element of the each QP run is stored as it represents the most recent position for the cyclist. The QP is then conducted for the new series of cyclist positions in the current PTI.

The QP does not use the optimization results from previous steps as equality constraints in the next step. Instead, it outputs a fresh final position from each time step. The reasons for this are as follows:

- 1) The optimized results could be derived from inconsistent detections, and feeding the inaccurate results to the next run of QP might accumulate more errors in the true positions;
- 2) Adding too many equality constraints can over-constrain the QP and thus deliver erroneous results.
- 3) It is better to keep the errors in each data point independent and to filter the noise in a second step than to accumulate biased errors that cause long-term drift and are difficult to correct.

When the first run of QP finishes (i.e., 15 samples have been accumulated), the Kalman filter is activated to smooth the data.

Each time there is a new estimate from the QP, the Kalman filter weighs this new measurement against the positions derived by the model and outputs a better estimate of the current position.

To model variation in the width of the cyclist when viewed from the side, the noise in detected distance is assumed to be a Gaussian white noise process with a standard deviation of 0.05m.

The examples below are used to show the performance of the Kalman filter. In the examples, the relative speed was 5km/h and the lateral distance started at 1.2m. The sampling rate was 7.5Hz and the size of each QP sample set was 15.

The parameters in the Kalman filter were tuned manually for a balanced performance for various relative speeds and manoeuvres. Fig 12 shows the trajectories of the cyclist and the sensor positions in the truck coordinate system. The relative motion is from left to right. The QP-only method generates an error exceeding 10cm at some points in time. The cyclist positions are not consistent longitudinally as if the cyclist moves back and forth, and these cannot be used in predicting the future position of the cyclist. The Kalman filter improves the position estimations by eliminating the longitudinal inconsistencies. At the beginning of the Kalman filtering process, the estimated positions are closer together because the initial velocity of the cyclist in the state vector is set to zero. With more measurement inputs to the Kalman filter, the estimation improves. The errors involved in cyclist positions are no greater than 5cm and this is tolerable for predicting the future positions of the cyclist.

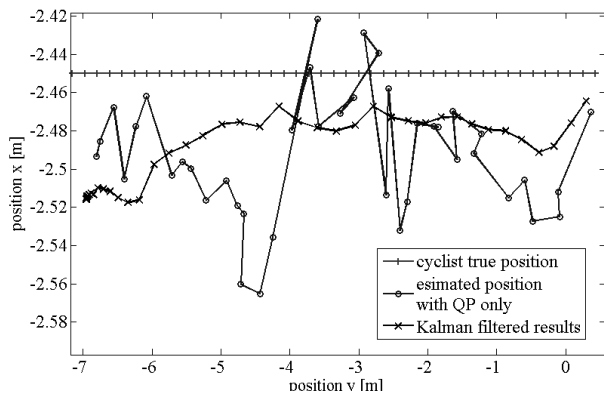


Fig. 12 Estimation results using QP only and QP with Kalman filter, cyclist 5kph faster than the HGV, cyclist parallel to HGV

Fig. 13 shows a case when the cyclist steers away from the HGV while maintaining all other parameters the same. The lateral speed of the cyclist is set to 0.1m/s. A smoother trajectory is estimated by Kalman filter. The position errors after Kalman filtering are considered to be sufficiently accurate for the position prediction step.

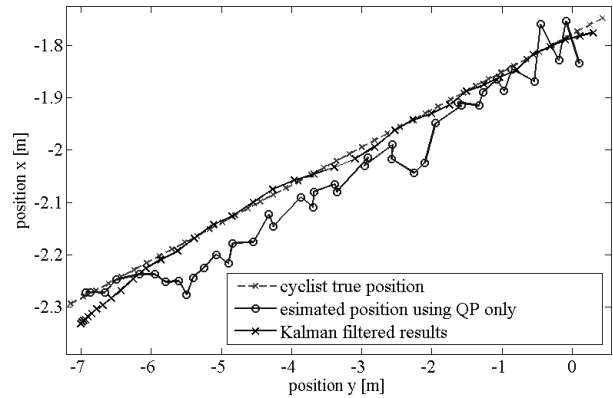


Fig. 13 Estimation results using QP only and QP with Kalman filter, cyclist 5kph faster than the HGV, getting closer to the front end of HGV

#### IV. EXPERIMENTAL MEASUREMENTS

Twelve ultrasonic sensors were mounted onto the left side of a 4 axle Scania tipper, with a gap between sensors being 0.8m (see Fig. 14). A real time signal analysis and control program was developed using Simulink Real Time (formerly known as 'xPC target'). The solver for QP and the Kalman filter were coded in an Embedded MATLAB function to perform the calculations in real-time. A dummy cyclist mounted on a moving platform was used during the test and followed a specified speed profile. Details of the testing set up and procedures are described in [11] and [27].

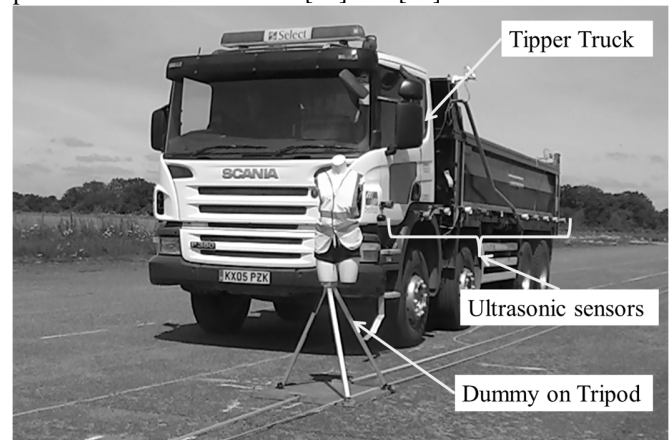


Fig. 14 Testing set up for experimental measurements

Various dummy speeds were used, with the maximum speed differential set to 5km/h. A speed differential exceeding 5km/h would result in loss of detections by the experimental ultrasonic sensors used in the prototype system [11].

An example is provided in Fig. 15 which has a dummy speed of 3km/h. It is noticeable that Kalman filter (black crosses) significantly reduces estimation errors of the QP. The maximum error in lateral position is approx. 5cm.

The standard deviation of the estimation errors and maximum detection errors for all five different relative speeds are provided in Table 1. These results demonstrate that the real time processing system can track the dummy to an acceptable level of accuracy.

It is important to check whether similar performance could be

achieved when cyclists moves at an angle relative to the truck. Fig. 16 shows the estimated positions using QP with Kalman filter for the dummy moving at various speeds. The error characteristics are summarized in Table 2. The results show a similar level of accuracy to the parallel case for relative speeds up to 5km/h, with RMS errors less than 5cm for relative speeds up to 5km/h.

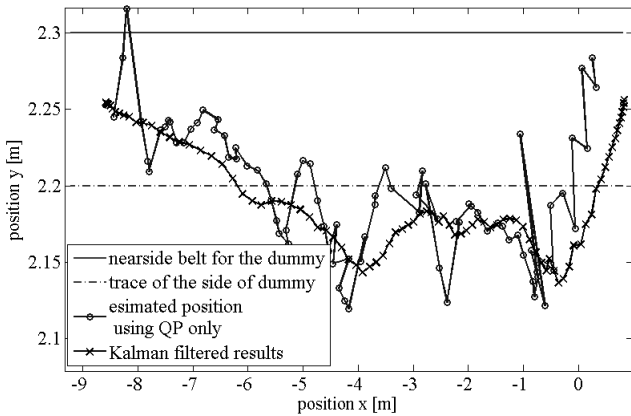


Fig. 15 Testing result of a moving dummy at 3km/h in parallel with a stationary truck

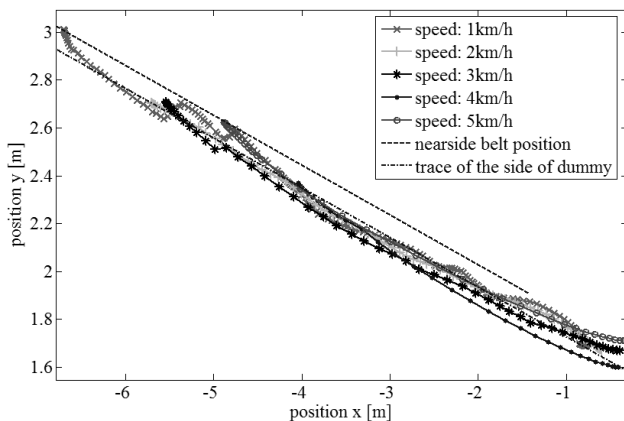


Fig. 16 Estimated position comparisons for different speeds for the dummy travelling diagonally

The limited range of differential speeds possible is a result of low sampling rate possible with the experimental ultrasonic sensors. This paper aims to determine the feasibility of the approach – not to demonstrate a market-ready system. Alternative suppliers are approached to develop ultrasonic sensors with higher sampling rates.

Quadratic programming is often regarded as computationally intensive and various methods [28] have been described to enhance its performance in real time. A primal-dual quadratic solver was written and implemented in Simulink. Based on profiling results of real time execution on a real-time prototyping system (2.6GHz Intel Core processor for target machine), it takes around 4.2ms maximum to complete the QP process, and another 0.1ms to complete all other tasks. Since the sampling rate of sensors is 7.5Hz, all calculations need to be done in 130ms. This means only about 3% of the allowed computation time is used, thus offering a sufficient computation margin.

## V. CONCLUSIONS

This paper describes algorithms for estimating the relative position and motion of a cyclist based on detection from a set of ultrasonic sensors mounted along the side of a lorry. This approach is the first of its kind to use ultrasonic sensor arrays for tracking cyclists moving alongside trucks, and more specifically, to perform position estimation using Quadratic Programming, which takes in distance information (one dimension) and outputs positions (two dimensions). The proposed package of methods does not require fusion with other sensory inputs.

The following conclusions can be drawn:

- 1) Quadratic programming is effective in estimating the cyclist position by optimising the bearing angle relative to the sensor. The objective in the QP is to minimise the deviation of the cyclist's longitudinal acceleration from a constant value. The constant acceleration model for the QP works better than the constant velocity model in cases when there is no *a priori* knowledge of the cyclist motion. The constant velocity model provides good accuracy and requires significantly less computation.
- 2) A Kalman filter was designed to improve the estimation accuracy in the presence of sensor noise. It significantly improved the prediction accuracy.
- 3) Experimental tests with an array of twelve sensors mounted along the side of a lorry demonstrated that the combined system of QP and Kalman filter can estimate cyclist position with an RMS error of less than 5cm for either parallel or diagonal motion at relative velocities up to 5km/h. This is considered to be sufficiently accurate for implementation in an automated collision avoidance system. A wider range of relative speeds could be achieved for sensors that operate at a higher sampling frequency.
- 4) The system is designed for real time operation, and the tests with the demonstrator proved that QP process can be made to work in real time.

## VI. ACKNOWLEDGEMENTS

The authors thank the support of the Cambridge Vehicle Dynamics Consortium, whose member at the time of writing are: Anthony Best Dynamics, Brigade Electronics, Camcon, Cambridge University, Denby Transport, Firestone Goodyear, Haldex, Laing O'Rourke, MIRA, SDC Trailers, SIMPACK, Tridex BV, Tinsley Bridge, Wincanton and Volvo Trucks. Special thanks go to Anthony Best Dynamics and Laing O'Rourke for providing essential testing equipment. Thanks also go to Dr Richard Roebuck, Dr Leon Henderson and Dr Amy Rimmer for their assistance with the testing. The authors also would like to thank China Scholarship Council and Cambridge Trusts for their contribution to the researching fund.

## VII. TABLES

Dummy speed relative to the stationary truck (in km/h)	Mean lateral errors (in cm)	Standard deviation of lateral errors (in cm)
1	-1.3	4.0
2	-0.7	3.6
3	1.0	4.1
4	0	4.8
5	2.9	3.4

Table 1 Position estimation accuracy for cyclist moving in parallel with a stationary truck

Dummy speed relative to the stationary truck (in km/h)	Mean lateral errors (in cm)	Standard deviation of lateral errors (in cm)
1	-0.1	4.3
2	0.2	2.3
3	1.1	2.8
4	1.8	3.4
5	-0.6	1.0

Table 2 Position estimation accuracy for cyclist moving diagonally w.r.t. a stationary truck

## REFERENCES

- [1] "Reported Road Casualties Great Britain: 2013 Annual Report," Department for Transport, London, UK25 September 2014.
- [2] T. L. Robinson and W. Chislett, "Commercial vehicle safety priorities-ranking of future priorities in the UK," Transport Research Laboratory, London SO601N7, March 2010.
- [3] S. Nedevschi, S. Bota, and C. Tomiuc, "Stereo-Based Pedestrian Detection for Collision-Avoidance Applications," *IEEE Transactions on Intelligent Transportation Systems*, vol. 10, pp. 380-391, 2009.
- [4] W. Tian and M. Lauer, "Fast Cyclist Detection by Cascaded Detector and Geometric Constraint," in *2015 IEEE 18th International Conference on Intelligent Transportation Systems*, 2015, pp. 1286-1291.
- [5] X. Li, L. Li, F. Flohr, J. Wang, H. Xiong, M. Bernhard, *et al.*, "A Unified Framework for Concurrent Pedestrian and Cyclist Detection," *IEEE Transactions on Intelligent Transportation Systems*, vol. 18, pp. 269-281, 2017.
- [6] Volvo, "Volvo Car Group introduces world-first Cyclist Detection with full auto brake ", ed, 2013.
- [7] Brigade Electronics, "Backeye@360 360° Camera Monitor Systems," ed. South Darenth, Kent, UK, 2014, p. 2.
- [8] "Safer Lorry Scheme Class V and VI Mirrors," T. f. London, Ed., ed. London, 2014.
- [9] Daimler AG. (2016). *New Mercedes-Benz Sideguard Assist: More safety in urban traffic*. Available: <https://www.daimler.com/innovation/safety/sideguard-assistant.html>
- [10] Y. Jia and D. Cebon, "A strategy for avoiding collisions between heavy goods vehicles," *Proceedings of the Institution of Mechanical Engineers, Part D: Journal of Automobile Engineering (in press)*, 2017.
- [11] Y. Jia, "An Automated Cyclist Collision Avoidance System for Heavy Goods Vehicles," Ph.D. thesis, Department of Engineering, University of Cambridge, Cambridge, 2014.
- [12] N. I. Giannoccaro, L. Spedicato, and C. d. Castri, "A New Strategy for Spatial Reconstruction of Orthogonal Planes Using a Rotating Array of Ultrasonic Sensors," *IEEE Sensors Journal*, vol. 12, pp. 1307-1316, 2012.
- [13] D. Bank, "A novel ultrasonic sensing system for autonomous mobile systems," in *Proceedings of IEEE Sensors*, 2002, pp. 1671-1676 vol.2.
- [14] L. Gu, X. Kou, and J. Jia, "Distance measurement for tower crane obstacle based on multi-ultrasonic sensors," in *2012 IEEE International Conference on Automation Science and Engineering (CASE)*, 2012, pp. 1028-1032.
- [15] H. Dai, S. Zhao, Z. Jia, and T. Chen, "Low-Cost Ultrasonic Distance Sensor Arrays with Networked Error Correction," *Sensors (Basel, Switzerland)*, vol. 13, pp. 11818-11841, 2013.
- [16] Cui H., Song J., and L. D., "Ultrasonic Array Based Obstacle Detection in Automatic Parking," in *Proceedings of 2013 Chinese Intelligent Automation Conference*, 2013.
- [17] B. D. V. Veen and K. M. Buckley, "Beamforming: a versatile approach to spatial filtering," *IEEE ASSP Magazine*, vol. 5, pp. 4-24, 1988.
- [18] C. H. Lampert, M. B. Blaschko, and T. Hofmann, "Beyond sliding windows: Object localization by efficient subwindow search," in *2008 IEEE Conference on Computer Vision and Pattern Recognition*, 2008, pp. 1-8.
- [19] J. Tompson, R. Goroshin, and A. Jain, "Efficient object localization using Convolutional Networks," presented at the 2015 IEEE Conference on Computer Vision and Pattern Recognition (CVPR), Boston, MA, USA, 2015.
- [20] B. Fulkerson, A. Vedaldi, and S. Soatto, "Class segmentation and object localization with superpixel neighborhoods," in *2009 IEEE 12th International Conference on Computer Vision*, 2009, pp. 670-677.
- [21] A. Kassim, "Innovative techniques for analyzing cyclist behaviour and predicting cyclist safety," PhD, Carleton University, 2014.
- [22] S. Zernetsch, S. Kohnen, M. Goldhammer, K. Doll, and B. Sick, "Trajectory prediction of cyclists using a physical model and an artificial neural network," in *2016 IEEE Intelligent Vehicles Symposium (IV)*, 2016, pp. 833-838.
- [23] E. A. I. Pool, J. F. P. Kooij, and D. M. Gavrila, "Using road topology to improve cyclist path prediction," in *2017 IEEE Intelligent Vehicles Symposium (IV)*, 2017, pp. 289-296.
- [24] G. Krieger, N. Gebert, and A. Moreira, "Multidimensional Waveform Encoding: A New Digital Beamforming Technique for Synthetic Aperture Radar Remote Sensing," *IEEE Transactions on Geoscience and Remote Sensing*, vol. 46, pp. 31-46, 2008.
- [25] R. D. C. Monterio and I. Adler, "Interior path-following primal dual algorithms, Part II: Convex quadratic programming," in *Math.Prog.44*, 1989, pp. 45-66.
- [26] G. Welch and G. Bishop, *An introduction to the Kalman filter*. University of North Carolina at Chapel Hill, Department of Computer Science, Chapel Hill, NC 27599-3175, 2001.
- [27] Y. Jia and D. Cebon, "Field testing of a cyclist collision avoidance system for heavy goods vehicles," *IEEE Transactions on Vehicular Technology*, vol. PP, 2016.
- [28] S. Boyd and J. Mattingley, *Automatic Code Generation for Real-Time Convex Optimization*. Cambridge: Cambridge University Press, 2010.

**Yanbo Jia** received the B.S. degree in Automotive Engineering from Jilin University, Changchun, Jilin Province, China, in 2009 and Ph.D. degree in Engineering in 2015 from University of Cambridge, Cambridge, UK.

He becomes the Research Associate in Cambridge University Engineering Department since March 2015. His research is focused on collision avoidance between cyclists and heavy goods vehicles, which covers sensors, signal processing, algorithm development, real-time system design and product prototyping.

**David Cebon** received BE in mechanical engineering from University of Melbourne, Australia in 1980 and PhD degree in engineering from University of Cambridge, UK, in 1985.

He has been employed by the University of Cambridge since 1985, first as a lecturer and more recently as professor of mechanical engineering. His research covers the mechanical, civil, and materials aspects of road transport engineering. He has authored or co-authored more than 150 papers on dynamic loads of heavy vehicles, road and bridge response and damage, advanced suspension design for heavy vehicles, heavy vehicle safety, mobility and fuel consumption and the micromechanics

of asphalt deformation and fracture.

Prof. Cebon is a Fellow of the Royal Academy of Engineering and the Institution of Mechanical Engineers. He is Director of the Cambridge Vehicle Dynamics Consortium and the Centre for Sustainable Road Freight and he leads Cambridge University Engineering Department's Transport Research Group and the Engineering Department's research theme 'Energy, Transport and Urban Infrastructure'. He serves on the Editorial Boards of three international journals.